

# RADIOACTIVE HALOS<sup>1</sup>

x 5541

Robert V Gentry

Chemistry Division, Oak Ridge National Laboratory, Oak Ridge, Tennessee

## CONTENTS

(NOTE: PAGE NUMBERS HAVE BEEN MODIFIED TO REFLECT THIS PUBLICATION OF THE DOCUMENT)

INTRODUCTION	1
THE RADIOACTIVE ORIGIN AND PROVENANCE OF HALOS	1
EVIDENCE FOR CONSTANCY OF RADIOACTIVE DECAY ENERGIES OVER GEOLOGIC TIME	3
VARIAN HALOS AND EVIDENCE FOR UNKNOWN RADIONUCLIDES	5
<i>Polonium Halos</i>	5
<i>Photographic evidence</i>	5
<i>Comparison of Po halo radii and CB sizes</i>	5
<i>Genesis, geophysical implications, and question of isomer precursors</i>	5
<i>Dwarf Halos</i>	6
<i>X Halos and Other Intermediate Size Varieties</i>	7
Giant Halos and Unknown s-Radioactivity	7
Mass Analysis of Halo Inclusions	8

## INTRODUCTION

In some thin samples of certain minerals, notably mica, there can be observed tiny aureoles of discoloration which, on microscopic examination, prove to be concentric dark and light circles with diameters between about 10 and 40  $\mu$ m and centered on a tiny inclusion. The origin of these halos (first reported between 1880 and 1890) was a mystery until the discovery of radioactivity and its powers of coloration; in 1907 Joly (1) and M $\ddot{u}$ gge (2) independently suggested that the central inclusion was radioactive and that the  $\alpha$ -emissions from it produced the concentric shells of coloration (the circular patterns observed in thin sections are, of course, simply plane sections through concentric spheres). The earliest name, "pleochroic halos," was partially a misnomer, since halos were later found in isotropic minerals which do not show pleochroism.

Aside from their interest as attractive mineralogical oddities, halos command attention because they are an integral record of radioactive decay in minerals that constitute the most ancient rocks. Most importantly, this thermal-resistant record is detailed enough to allow estimation of the decay energies involved and to identify the nuclides decaying (through the energies and through genetic connections). This latter possibility is particularly exciting because classes of halos exist which correspond to no known radionuclide. Barring the possibility of a nonradioactive origin, these are evidence for hitherto undiscovered or presently extinct radionuclides. Joly, a geology professor at Dublin, lost nearly all his halo evidence for an element he called "hibernium" in the Easter uprising of 1916.

<sup>1</sup>Research sponsored by the US Atomic Energy Commission under contract with Union Carbide Corporation. RVG is a guest scientist at ORNL from Columbia Union College, Takoma Park, Maryland.

This review of halos and their bearing on nuclear science is organized into three main sections covering: the radioactive origin and provenance of halos, evidence for constancy of radioactive decay energies over geologic time, and variant halos and evidence for unknown radionuclides.

## THE RADIOACTIVE ORIGIN AND PROVENANCE OF HALOS

Evidence to support the Joly-M $\ddot{u}$ gge hypothesis of a radioactive origin of halos is both analytical and synthetic. The correspondence between halo dimensions and the ranges of typical alpha particles (extrapolated from air to mica) is suggestive of a causative connection, and an even stronger qualitative argument is the correspondence between the number of  $\alpha$ -emitters in the <sup>238</sup>U (or <sup>232</sup>Th) series and the number of rings in a corresponding halo. Schematic drawings (based on air  $\alpha$ -ranges) of a <sup>238</sup>U halo (Figure *la*) and a <sup>232</sup>Th halo (Figure *lb*) may be compared with halo photomicrographs in Figures *lc* and *ld* respectively. This illustrates rather well the compelling evidence of the patterns. Quantitative evidence about the patterns will be described after noting the synthetic evidence.

Rutherford (3) and Joly & Rutherford (4) provided synthetic evidence by showing that  $\alpha$ -radioactivity could produce halo-like coloration in solids. Rutherford (3) in 1910 reported that radon enclosed in a soda-lime glass capillary tube produced a colored annulus whose depth approximated the range of radon alphas in glass. In 1913, Joly & Rutherford (4) reported that a dose of  $1.5 \times 10^{13}$   $\alpha$ -particles/cm<sup>2</sup> produced a halo-like coloration in biotite (an Fe-rich mica).

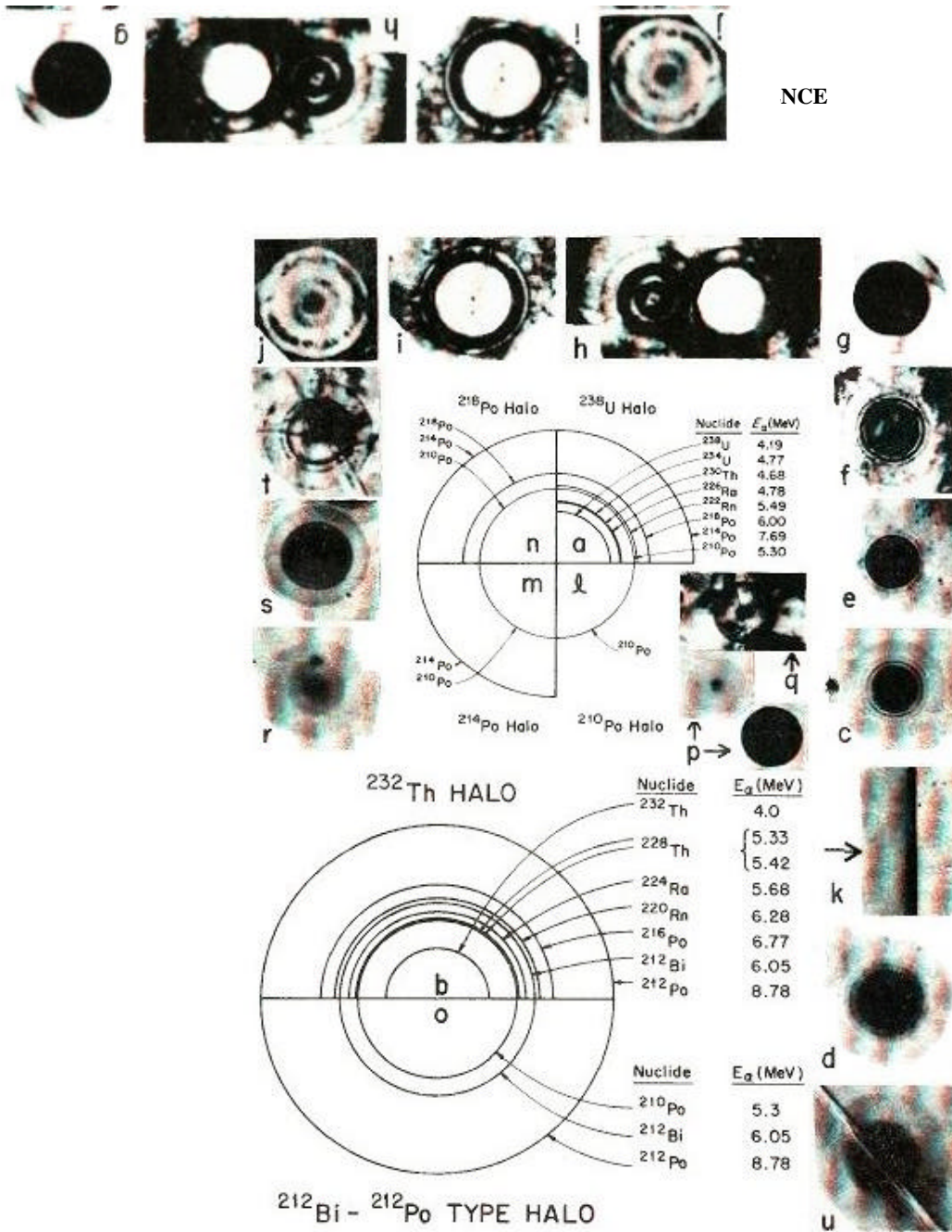


**Figure 1** The scale for the photomicrographs is 1 cm equivalent to 45 mm. (a) Schematic drawing of  $^{238}\text{U}$  halo with radii proportional to  $\alpha$ -ranges in air. (b) Schematic drawing of  $^{232}\text{Th}$  halo. (c)  $^{235}\text{U}$  halo in biotite formed by sequential  $\alpha$ -decay of the  $^{238}\text{U}$  decay series. (d)  $^{232}\text{Th}$  halo in biotite. (e) Embryonic  $^{238}\text{U}$  halo in fluorite. (f) Well-developed  $^{238}\text{U}$  halo in fluorite. (g) Overexposed  $^{238}\text{U}$  halo in fluorite showing inner ring diminution. (h) Two overexposed  $^{238}\text{U}$  halos in fluorite showing inner ring radius diminution in one halo and obliteration in the other. (i) Further overexposed  $^{238}\text{U}$  halo in fluorite showing outer ring reversal effects. (j) Second stage reversal  $^{238}\text{U}$  halo in fluorite. Rings not related to  $^{235}\text{U}$   $\alpha$ -emitters. (k) Coloration band formed in mica by 7.7 MeV  $^4\text{He}$  ions. Arrow shows direction of beam penetration. (l) Schematic of  $^{210}\text{Po}$  halo. (m) Schematic of  $^{214}\text{Po}$  halo. (n) Schematic of  $^{218}\text{Po}$  halo. (o) Schematic of  $^{212}\text{Bi}$ - $^{212}\text{Po}$  halo. (p) Two  $^{210}\text{Po}$  halos in biotite, one light and one very dense. (q)  $^{210}\text{Po}$  halo in fluorite. (r)  $^{214}\text{Po}$  halo in biotite. (s)  $^{218}\text{Po}$  halo in biotite. (t)  $^{218}\text{Po}$  halo in fluorite. (u)  $^{212}\text{Bi}$ - $^{212}\text{Po}$  type halo in biotite.

Quantitative evidence results from using newer methods that permit observation of single fission tracks in biotite (Fleischer, Price & Walker 5). After appropriate etching, an embryonic U halo (only first ring visible) exhibits a cluster of 20 to 30  $^{238}\text{U}$  fossil fission tracks (Gentry 6), implying that  $\sim 5 \times 10^7$   $^{238}\text{U}$  atoms have decayed ( $I_a/I_f = 2 \times 10^6$  for  $^{238}\text{U}$ ). Thus at the first U ring radius of 13 mm the natural  $\alpha$ -dose approximates that determined by Joly & Rutherford (4). This limited agreement in diverse samples is accidental, for, as Picciotto & Deutsch (7) have shown, different biotites may show wide coloration threshold responses.

By irradiating halo-containing biotites with  $^4\text{He}$  ions Gentry (6, 8) found the natural and induced coloration thresholds compare favorably enough to suggest that for some biotites reciprocity is a valid principle (i.e. discoloration is approximately independent of dose rate up to an  $\alpha$  flux of  $10 \text{ nA/mm}^2$ ). Furthermore, coloration reversal effects arising from and occurring adjacent to highly radioactive inclusions (Figure 2c) have been duplicated by high-dose exposures (7). However, other halo reversal effects suggest reciprocity is not uniformly applicable. For example, in certain samples coloration inversion occurs immediately exterior to the halo ring terminus, thus accentuating the halo ring structure (Figures 1c, d). Generally this effect is not observed in briefly irradiated (0.1 to 30 min) samples of biotite or fluorite. This experimental approach to halo coloration as pursued by Hövermann (9), Poole (10), Prizbram (11), Ramdohr (12), and others (3, 4, 6—8), informative as it has been, has not been paralleled by an equivalent amount of theoretical work.

Now halos generally occur in an igneous environment and even in some igneous fragments that occasionally occur interspersed in sedimentary rocks (Stark 13). An exception is their occurrence in coal and asphaltized wood (Jedwab 14). While mineralogists have found over 40 minerals in which halos occur, their distribution within these minerals is very erratic (12, 13). Further, halos in opaque minerals, such as ilmenite, are of course visible only in reflected light and exhibit poorly defined ring structure, partly due to smearing effects produced by large (? 10 mm) halo inclusions (Ramdohr 12). Only those minerals that are transparent in 30-mm thin section are suitable for detailed ring analysis. Even in these considerable microscopic scanning time is required to locate good halo specimens.

Ease of thin section preparation and fairly good registration properties have made biotite an ideal choice for several halo investigations (namely Joly 15, van der Lingen 16, Wiman 17, Imori & Yoshimura 18, Kerr-Lawson 19, Henderson et al 20, and Gentry 6, 8). The three-dimensional nature of a halo is demonstrated when a biotite specimen is prepared for microscopy. Because of its perfect cleavage properties, the leaves of a book of mica are easily separated with Scotch tape, each successive section revealing a ring pattern of increasing size until the diametral section is obtained. Ring sizes must be measured with diametral sections, and most accurate measurements result from specimens having exceptionally small nuclei.

As good as some halos in certain biotite specimens are, the investigations of Hirschi (21), Gudden (22), Schilling (23), and Gentry (24) have shown that fluorite halos afforded even better microscopic resolution of the halo rings. Mahadevan

(25) has shown that halos in cordierite may also yield suitable ring structure for accurate radii measurement.

The halo inclusions occur as accessory minerals and have been identified as zircon, xenotime, monazite, allanite, sphene, apatite, uraninite, and thorite (Joly 15, Ramdohr 12, Hutton 26, Snetsinger 27, and Gentry 8, 28). However, their small size sometimes prevents use of petrologic identification techniques.

Uranium, Th, and other specific halo types have been observed mainly in Precambrian rocks (6, 8, 15, 17—20, 28), but much yet remains to be learned about their occurrence in rocks from other geological periods. Mineralogical studies have shown halos do exist in rocks stretching from the Precambrian to the Tertiary Periods (13, Holmes 29), but unfortunately the halo type existing in these formations was not identified by ring structure.

### EVIDENCE FOR CONSTANCY OF RADIOACTIVE DECAY ENERGIES OVER GEOLOGIC TIME

Because radiohalos are integral  $\alpha$ -radiographs, an early interest was to ascertain whether U and Th halo radii were of the same size in rocks from different geological periods. Any unaccounted for non-uniformity would imply different decay energies and perhaps suggest a different value of  $\lambda$ , the decay constant. Such investigations were based on the premise that well-defined halo rings could be associated with specified  $\alpha$ -energies.

Joly, perhaps not realizing all the subtle factors which may influence halo radii sizes, announced in 1923 that U halo radii were indeed variable in rocks from different geological periods and suggested this was evidence for a change in  $\lambda$ . In 1926-1927, other investigators (18, 19, 23) reported that U and Th halo radii in biotite, cordierite, and fluorite approximated the expected values. However, these measurements were made on halos within the same host rock and did not in themselves counter Joly's claim of variable halo radii in rocks from different epochs.

Even so, Kerr-Lawson (19) made an important observation. In very thin biotite flakes, he saw the inner  $^{238}\text{U}$  ring resolved from the subsequent U halo rings (see Figure 1a, c). Since Joly (15) had not reported this inner ring, Kerr-Lawson inferred Joly's halo mineral sections were too thick to permit good ring resolution and attributed Joly's variable halo radii to a confusion in measuring the inner U halo rings. Personal examination of some of Joly's thin sections has confirmed this point.

In the 1930s Henderson and co-workers (20) performed a classic series of experiments using a halo photometer for direct recording of halo ring patterns. With little theoretical justification Henderson et al (20) compared [as had others (15, 18, 19)] halo ring sizes with the minima of the composite curve formed by superimposing all the  $^{238}\text{U}$  decay chain Bragg ionization curves. There were inherent problems because a single composite curve could at best represent only one of the many halo growth stages. Yet this approach seemed partially successful, for the composite curve (uncorrected for inverse square effect) did resemble the photometric scan of a U halo which showed all rings (Figure 1c). However, when corrected for the inverse square effect, the peaks and valleys in the curve

previously associated with the halo rings became almost nonexistent. Clearly it is not possible to obtain reliable standards for radii comparison using this procedure.

Further attempts to compare halo radii with equivalent mineral ranges derived from  $\alpha$ -ranges in air (20) are also unsatisfactory because of uncertainties in the air-mineral conversion factor. Comparison of halo radii with  $\alpha$ -ranges calculated from the Bragg-Kleeman (or a similar) relation is possible, but necessarily assumes that ring coloration extends the full  $\alpha$ -range. Now newer techniques do allow appropriate standards to be developed, but before discussing these we first digress to examine in more detail halos in different growth stages.

Radiohalos in fluorite will be used as examples. Figure 1k shows an embryonic U halo wherein only the first two rings are prominent. Figure 1f shows the normal or intermediate stage U halo wherein all rings may be detected. The U halo in Figure 1g is overexposed in the inner halo region, resulting in coloration reversal and the formation of a diminutive ghost ring in the center. Figure 1h shows two other partially reversed U halos, one of which shows the diminutive inner ring, while the other has experienced complete obliteration of all the inner rings. The U halo in Figure 1i is even more overexposed, and encroaching reversal effects have given rise to another ghost ring just inside the outermost periphery. Figure 1j shows a still more highly overexposed U halo in which second-stage reversal effects have produced spurious ghost rings that are unrelated to the terminal  $\alpha$ -ranges.

Tracing out the above pattern of U halo development in fluorite is no straightforward task. Only by observing differential growth increments in thousands of halos (produced of course by differential amounts of U in the halo inclusions) is it possible to construct the sequence shown. Earlier investigators (12, 23) as well as a later one (Gentry 28, 30) at one time erred in inventing new  $\alpha$ -activity to account for some of the aforementioned ghost rings. Clearly a one-to-one correspondence between halo radius and  $\alpha$ -energy is not always valid.

We return to the discussion of the constancy of  $\alpha$ -decay energies and the problem of developing reliable standards for halo radii comparisons. The most direct technique is to irradiate halo-containing minerals with a sufficient dose of monoenergetic  $^4\text{He}$  ions until halo-like coloration develops (Gentry 8, 24). If reciprocity holds, the  $^4\text{He}$  ions will produce a coloration band (see Figure 1k) that in theory is equivalent in depth or size to a halo radius produced by the same energy  $\alpha$ -particles. These induced coloration band (CB) sizes then form the standards against which halo radii may be compared. [Interestingly a densitometer profile of the CB in Figure 1k shows a marked resemblance to the shape of the Bragg ionization curve, thus providing some basis for the superposition procedure used by Henderson (20) and Joly (15).] However, the actual comparison procedure requires that certain additional factors be considered.

First, in some minerals, especially biotite, this reviewer has found that halo radii are somewhat dose dependent; darker rings show slightly higher radii than faint rings (24). (CB sizes show a similar effect, implying coloration intensities in natural

and induced specimens should be matched before size comparisons are made.) This dose effect is often masked by subtle halo radius variations produced by attenuation of the  $\alpha$ s emitted within the inclusion itself. For example, when the inclusion (e.g. zircon) is more dense than the host mineral (e.g. biotite), slightly smaller radii result in embryonic halos; extreme values are reached only after a heavy dose. However, a heavy dose means a dark halo which tends to obscure the inner halo rings, making measurements difficult.

Although the finite inclusion size renders all radii measurements uncertain to a degree, there are two cases when this correction is minimized. For *densely colored* halos surrounding large inclusions (e.g. see Figure 2), the only reasonable radius measurements are those made from the inclusion edge. In the other case for halos in biotite with only tiny 1-mm inclusions, this reviewer arbitrarily makes no correction for inclusion size.

In fluorite the situation is different. Here the effect of finite inclusion size is minimized because some halos exist with nuclei only 0.5  $\mu\text{m}$  or less in diameter. Yet in contrast to halos in biotite, there is evidence that in some cases radioactivity is superficially distributed on the inclusion, implying halo radii be measured from the inclusion edge. Fortunately, the halo ring size in this mineral is only very minimally dependent on a dose so that even embryonic halo rings form a practically maximum size (22—24).

Table I shows U halo radii measurements in biotite, fluorite, and cordierite (19, 20, 23—25) as well as CB sizes produced by accelerator  $^4\text{He}$  ion beams of varying energy in the same minerals (Gentry 24). Note that the comparison between fluorite CB sizes and halo radii is quite good, while in biotite the halo radii are somewhat smaller than the equivalent CB sizes. As discussed earlier, this deviation in biotite is likely due to the effects of a finite inclusion size plus the dose-dependent radius effect rather than a change in  $\alpha$ -energy.<sup>2</sup> Note also the comparison between CB sizes and halo radii in cordierite. Here the agreement is fair even though the U halos in cordierite possessed large inclusions, necessitating that halo radii be measured from the inclusion edge (Mahadevan 25).

Interestingly densitometer profiles of some of my U halos show the same small halo rings that Henderson (20) noted, but these appear to be only artifacts of the coloration process and are not included in Table I.

With respect to the decay rate question, Spector (31) has argued that the differences between Henderson et al (20) halo radii measurements and equivalent air mineral ranges present a case for a variable  $\lambda$ . In the light of the above experimental uncertainties, this conclusion is not necessarily valid. On the other hand, Gentry (24) has shown that even exact agreement between halo radii and corresponding CB sizes does not necessarily imply an invariant  $\lambda$  and in fact uncertainties in radius measurements alone preclude establishing the stability of  $\lambda$  for  $^{238}\text{U}$  to more than 35%.

<sup>2</sup> My U halo radii in mica show in the G column of Table 1 give the range of radii sizes in this particular mica.

**Table 1** Halo radii and induced coloration band (CB) size measurements <sup>a</sup>

<sup>4</sup> He Induced Coloration Band Sizes (mm)					E (MeV)	Nuclide	U Halo Radii (mm)						Po Halo Radii (mm) in Mica						Po Halo Radii (mm) in Fluorite		
Mica			Fluorite	Cordierite			Mica			Fluorite	Cordierite	<sup>210</sup> Po		<sup>214</sup> Po		<sup>218</sup> Po		<sup>210</sup> Po	<sup>218</sup> Po		
G <sub>L</sub>	G <sub>M</sub>	G <sub>D</sub>	G	G			K-L	H	G	S	G	M	H	G <sub>L,D</sub>	H	G <sub>L</sub>	H	G <sub>L,M</sub>	G	G	
?	?	?	?	?	?	?	?	? <sub>0</sub>	?	?	?	?	?	?	?	?	?	?	?	?	?
13.4	13.8	14.2	14.1	16.2	? 4.2	<sup>238</sup> U?	12.3	12.7	12.2? 13.0	14.0	14.2	16		NP	NP	NP	NP	NP	NP	NP	
NM <sup>b</sup>	16.7	NM	17.3	19.2	? 4.77	<sup>226</sup> Ra?	15.4	15.3	14.9? 15.6	16.9	16.9	19		NP	NP	NP	NP	NP	NP	NP	
NM	NM	NM	NM	NM	? 4.66	<sup>230</sup> Th?	NR	NR	NR	NR	NR	NR		NP	NP	NP	NP	NP	NP	NP	
NM	16.7	NM	17.3	19.2	? 4.78	<sup>234</sup> U?	15.4	15.3	14.9? 15.6	16.9	17.1	19		NP	NP	NP	NP	NP	NP	NP	
NM	19.3	20.0	19.6	22.5	? 5.3	<sup>210</sup> Po?	NR <sup>c</sup>	NR	NR	19.3	19.5	NR	19.8	18.2? 19.9	20.0	18.3	19.9	18.1? 19.3	19.8	19.8	
NM	20.5	21.1	NM	NM	? 5.49	<sup>222</sup> Rn?	18.6	19.2	17.9? 18.8	20.5	20.5	23.5	NP	NP	NP	NP	NP	NP	NP	NP	
NM	23.0	23.9	23.6	26.7	? 6.0	<sup>218</sup> Po?	22.0	23.0	21.7? 22.2	23.5	23.5	26.5	NP	NP	NP	NP	24.0	22.5? 23.3	NP	23.7	
33.1	33.9	34.4	34.6	38.7	? 7.69	<sup>214</sup> Po?	33.0	34.1	31.0? 32.9	34.5	34.7	38.5	NP	NP	34.5	33.3	34.0	33.2? 34.0	NP	34.9	

<sup>a</sup> The symbols *K-L*, *H*, *S*, *M*, and *G* represent halo measurements by Kerr-Lawson, Henderson, Schilling, Mahadevan, and Gentry; *GL*, *GM*, and *GD* represent Gentry's measurements on light (*L*), medium (*M*) [dose 10 to 20 times coloration threshold], or dark (*D*) [~ 50 times coloration threshold] induced coloration bands. *GL...D* and *G...M* represent Gentry's measurements on light-to-dark and light-to-medium coloration halos respectively; halos with these designations were visually determined. Gentry's measurements were made with a filar micrometer that could be read to 0.07 pm. The estimated overall uncertainty was ±0.3 pm.

<sup>b</sup> NM = not measured.

<sup>c</sup> NR = not resolve.

<sup>d</sup> NR = not present.

## VARIANT HALOS AND EVIDENCE FOR UNKNOWN RADIONUCLIDES

Variant halos exhibit ring patterns different from either U or Th halos. Some are due to α-decay from known radionuclides while others present diverse ring structure unlike any known α-decay sequence. In this reviewer's opinion unusual size halos present a most interesting challenge for geochemistry, nuclear science, and cosmology.

### Polonium Halos

**PHOTOGRAPHIC EVIDENCE** Figure 1*l*, *m*, *n*, *o* shows schematic drawings of several Po halo types. Note that those in Figure 1*l*, *m*, *n* exhibit only Po rings and are designated by the first (or only) Po α-emitter in the decay sequence. Note also these Po α-emitters are end members in the <sup>238</sup>U decay chain. The similarity between these schematics and the actual photographs in Figure 1 is easily seen; i.e. compare Figure 1*l* with Figure 1*p*, *q*; Figure 1*m* with 1*r*; and Figure 1*n* with 1*s*, *t*. Figure 1*o* shows a combination <sup>212</sup>Bi-<sup>212</sup>Po halo, which also has a <sup>210</sup>Po ring that is difficult to see in the photograph in Figure 1*u*. (Note this inner ring is not due to <sup>228</sup>Th α-decay because sequential decay rings are missing.)

Figure 1*q* shows a <sup>210</sup>Po halo in fluorite. The two slightly different size <sup>210</sup>Po halos in Figure 1*p* well illustrate the dose effect on halo radius in biotite. Figure 1*r* shows a <sup>214</sup>Po halo in biotite that approximately matches the coloration of the light <sup>210</sup>Po halo in 1*p*. In these cases the <sup>210</sup>Po halo radii agree well. Likewise the dark inner <sup>210</sup>Po ring in the <sup>215</sup>Po halo shown in Figure 1*s* compares well in size with the dark <sup>210</sup>Po halo in 1*p*.

Figure 1*t* shows a <sup>218</sup>Po halo in fluorite. Here an important observation can be made. Note that the annulus between the <sup>210</sup>Po and <sup>218</sup>Po rings in Figure 1*t* (cf Figure 1*n*) is distinctly wider than the same annulus in the <sup>238</sup>U halo in 1*f*. This is clear evidence that the <sup>222</sup>Rn ring in Figure 1*f* is missing from the halo in it. In other words, the halo in Figure 1*t* indeed originated with <sup>218</sup>Po rather than <sup>222</sup>Rn α-decay.

**COMPARISON OF PO HALO RADII AND CB SIZES** Table 1 gives measurements of Po halos in biotite and fluorite by Gentry (24) and Henderson et al (32). Henderson's measurements were made using the halo photometer, while the rest were made with a micrometer ocular. For comparison purposes I include measurements of some Po halos in biotite that exhibit radius variations due to dose effects. As Table 1 shows, the correspondence between Po halo radii and induced CB sizes leaves little doubt the Po halo ring structure does indeed match the respective Po α-emitters. Note the very good agreement between Po and <sup>238</sup>U halo radii in fluorite. In biotite the <sup>238</sup>U halo radii must be compared with very light Po halos in order to minimize radii differences from dose effects. Although not shown in Table 1, Po halo radii measurements in cordierite (25) also agree with CB sizes.

**GENESIS, GEOPHYSICAL IMPLICATIONS, AND QUESTION OF ISOMER PRECURSORS** Because Schilling (23) saw Po halos located only along cracks in his Wolsendorf fluorite sample, he suggested they originated from preferential deposition of Po from U-bearing solutions. [I have also found them separated from conduits (Figure 1*q*).] Later Henderson (32) invoked a similar but more quantitative hypothesis to explain

Po type halos along conduits in biotite. Those Po halos he found occurring apart from conduits (similar to those found by Gentry in Figure 1*p, r, s*) were more difficult to account for. Here a very qualitative laminar flow hypothesis was proposed. The intervention of World War II and his untimely demise soon thereafter prevented Henderson from determining whether these explanations were valid. [Although Henderson (32) suggested that such types existed, the halo in Figure 1*u* was discovered only recently by Gentry and cannot be explained on the basis of U daughter  $\alpha$ -activity alone.]

Now the reason for the various attempts to account for Po halos by some sort of secondary process is quite simple; the half-lives of the respective Po isotopes are far too short to be reconciled with slow magmatic cooling rates for Po-bearing rocks such as granites ( $T_{1/2} = 3$  min for  $^{218}\text{Po}$ ).

Yet Gentry (6), by using fission-track and  $\alpha$ -recoil techniques, found no evidence for a secondary origin of those Po halos in biotite, which occurred apart from conduits (cf Figure 1*p, r, s*). Consistent with the ring structure, fission-track analysis of the Po halo inclusions showed very little, if any, U. Further, the  $\alpha$ -recoil technique (Huang & Walker 33), which permits the observation of a single  $\alpha$ -recoil pit in biotite, was employed to measure the distribution of decayed  $\alpha$ -radioactivity in regions both adjacent to and far removed from Po halo inclusions. No differences in  $\alpha$ -recoil density were noted in the two areas. If U daughter  $\alpha$ -activity had fed the Po inclusions, a significantly higher  $\alpha$ -recoil density would have been in evidence.

One solution to this dilemma is the suggestion (24) that the parent nuclides of the Po in the halo inclusions were long half-life  $b$ -decaying isomers that may yet exist. Halo ring structure allows this, for  $b$ -radiation produces no coloration in halos in biotite, fluorite, or cordierite. [Laemmlein (34) reported  $b$ -halos in a certain quartz sample, but this is unconfirmed.] If such isomers existed, Po, U, and Th halos could all be explained by assuming that minute quantities of the respective nuclides were incorporated into separate halo inclusions either

before or coincident with the host rock crystallization.

### Dwarf Halos

Joly (15) reported the existence of dwarf halos with radii —  $\sim 5.2$  and  $8.5$  mm in the black micas from the pegmatite quarry at Ytterby near Stockholm. A rather unsatisfactory attempt has been made (7) to identify the 5.2-mm dwarf halo with  $^{147}\text{Sm}$   $\alpha$ -decay ( $E_{\alpha} = 2.24$  MeV). Dwarf halos are extremely rare and erratically distributed even in the few mica samples which contain them. Joly (15) considered their radioactive origin beyond question and attributed their bleached appearance to radiation overexposure or to elevated temperatures.

Gentry (28) has also found dwarf halos in a mica specimen from Ytterby, and the sizes are difficult to correlate with  $\alpha$ -decay systematics of known radioactive nuclides. The smallest dwarf halos range from only 1.5 to about 2.5 mm with associated  $\alpha$ -energies in the 1 MeV range (Figure 2*a*). The half-lives of known radionuclides are in excess of 10<sup>13</sup> years for  $\alpha$ -decay energies of 2 MeV or less. Such weakly active nuclides almost escape detection and would hardly be expected to produce a halo. Other dwarf halos with radii from 3 to 11 mm (Figure 2*b*) correspond to  $\alpha$ -energies of  $\sim 1.1$  to 3.4 MeV. Some of these dwarf halos reflect coloration differences possibly due to varying amounts of parent radionuclides in the inclusions. In this respect the occurrence of dual-ring dwarf halos also suggests a radioactive origin. Although Gentry has not yet seen dwarf halos in cordierite, Mahadevan's (25) report of equivalent dwarf sizes in this mineral lends much credence to the radioactive origin of such halos. Whether there exists a causal relation between the dwarf halos and the previously reported, though unconfirmed, low-energy  $\alpha$ -activity found by Bruki, Hernegger & Hilbert (35) is presently open to question. As noted earlier, the dwarf rings which Henderson (20) reported in some U halos appear to be only artifacts of the coloration process.

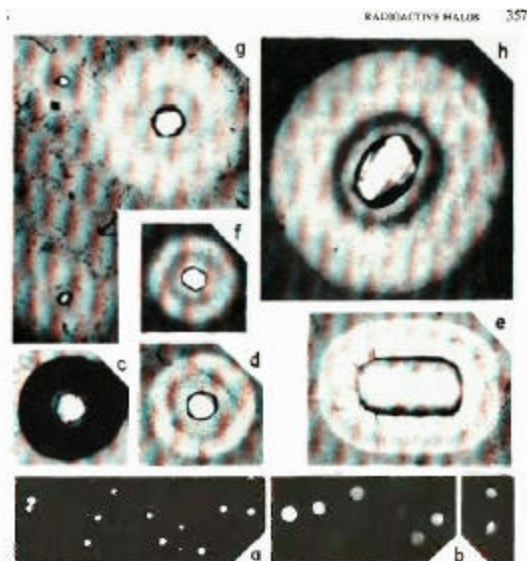


**Figure 2** The scale for all photographs is 1 cm = 50  $\mu$ m. (a) Dwarf halos (? 2-mm radius) in Ytterby mica. (b) Dwarf halos (3 mm?  $r$  ? 9 mm) in Ytterby mica. (c) Overexposed Th halo in ordinary biotite. (d) Th halo in Madagascar mica. (e) Th halo in Madagascar mica with a larger inclusion. (f) U halo in Madagascar mica. (g) Giant halo of ? 65-mm radius, and two light Th halos (Madagascar mica). (h) Giant halo of ? 90-mm radius, Madagascar mica.

### *X Halos and Other Intermediate Size Varieties*

Still rarer than the dwarf halos are the X halos first reported by Joly (15) in the micas from Ytterby and Arendal (Norway). Later van der Lingen (16) reported halos of similar dimensions occurred in a granite near Capetown. According to Joly (15) the inside ring of the X halo may be somewhat diffuse and measures about 8.5 to 9.8 mm in radius, corresponding to an  $E_a$  of about 2.9 to 3.2 MeV. The bleached rings extend out to a radius of about 14 to 15 mm, and sometimes an adjacent dark ring is evident at about 17 mm ( $E_a = 4.4$  to 5.0 MeV). The outer wide band extends to approximately 28 mm corresponding to an  $E_a$  of 6.7 to 6.9 MeV. Despite some similarities with the Th halo there is no known  $\alpha$ -decay sequence corresponding to these energies. Although well documented (and even photographed) by Joly, Gentry has yet to find any X halos in scanning thousands of sections of biotite from Ytterby, Arendal, and Capetown. Above all others, the search for this halo has taxed my eyesight. In this respect the much earlier (and quite obscure) reports (Schintimeister et al 36) of genetically related  $\alpha$ -decay of 3 MeV and 4.5 MeV are interesting, but they remain unconfirmed. Therefore any association with the very elusive X halo is only speculation.

Gentry (37) has reported the existence of a halo with rings apparently due to  $\alpha$ -energies of about 4.4 to 5.4 MeV. However, the relatively large size of the inclusion of this halo (6 mm in diameter) necessitates a re-examination of this halo with other techniques. Possibly the inner disc is a ghost ring resulting from  $\alpha$ -particle attenuation within the inclusion. If so, the halo may be the  $^{210}\text{Po}$  variety. I have also reported a halo possibly due to  $^{211}\text{Bi}$   $\alpha$ -decay (30). Thus far I found only two of these halos and more specimens are needed to confirm the identity of this type.

Another unusual halo was the so-called D halo reported by Henderson (32) to exhibit a diffuse boundary of radius  $\sim 16$  mm. He tentatively attributed this halo to  $^{226}\text{Ra}$   $\alpha$ -decay because the radius approximated the size of the  $^{226}\text{Ra}$  ring in the U halo. The absence of other rings, which should have appeared from daughter product  $\alpha$ -activity, was explained by assuming  $^{222}\text{Rn}$  diffused from the inclusion before it decayed. This, of course, is contrary to the situation observed in the normal  $^{238}\text{U}$  halo. Gentry has examined such halos, both in Henderson's original thin sections and in other biotites. They generally possess inclusions several microns in diameter and are without detailed ring structure. While they cannot be explained on the basis of  $^{226}\text{Ra}$   $\alpha$ -decay, the presence of fossil fission tracks indicates that U series  $\alpha$ -emitters produced part of the coloration in this halo type.

In addition to U and Th halos Iimori & Yoshimura (18) reported three halo sizes they designated as  $Z_1$ ,  $Z_2$ , and  $Z_3$  halos. These halos were attributed to actinium series  $\alpha$ -emitters. Gentry has examined some of the original slides as well as separate Japanese biotite samples in which such halos were reported. Gentry has observed that many halos in this biotite are very dark, so that it is necessary to prepare very thin sections in order that the halo inclusion can be seen. Some of the original sections containing Z halos were simply too thick to permit accurate halo radii measurements. In my opinion the  $Z_1$  and  $Z_2$  halos can be explained as U and/or combination U-

Th halos without postulating the actinium  $\alpha$ -emitters. The  $Z_3$  halo is actually a  $^{210}\text{Po}$  halo. In this context it should be noted that Joly's "emanation" halo was also a  $^{210}\text{Po}$  halo.

### *Giant Halos and Unknown $\alpha$ -Radioactivity*

Although Hirschi (21) was apparently the first to report giant halos, Wiman's (17) report of biotite halos with radii of 55 mm and 67 mm was better documented. Even so, on the basis of a rather cursory examination, Hoppe (38) was unable to confirm Wiman's results. Gentry (8), however, later found, after examining more than 1000 thin sections, that giant halos do exist in the rocks described by Wiman.

A more abundant source of giant halos was found in a mica from Madagascar. In this specimen Gentry (8) reported seven different groups of giant halos ranging from 45 mm to 110 mm. An unanswered question is whether these halos originate with high energy  $\alpha$ -emitters in the range from 9.5 MeV to 15 MeV. One group in particular with radii between 50 and 58 mm was tentatively attributed to the low-abundance (1:5500), high energy (10.55 MeV)  $\alpha$ -particles of  $^{212}\text{Po}$ , the last  $\alpha$ -emitter in the Th decay chain. Tentatively, this low-abundance group was associated with the 55-mm radius giant halo in the granites that Wiman studied. No other known nuclides occur with sufficient energy and/or abundance to produce the other groups of giant halos.

Therefore, seven other possibilities were considered (8) as explanations for the giant halos. These were: (a) Variations in  $\alpha$ -particle range due to structural changes in mica, (b) Diffusion of a pigmenting agent from the inclusion into the matrix, (c) Diffusion of radioactivity from the inclusion to the matrix, (d) Channeling, (e)  $\beta$ -radiation instead of  $\alpha$ -emission, (f) Long-range  $\alpha$ -particles from spontaneous fission, and (g)  $\alpha$ -particles or protons from ( $n, \alpha$ ) or ( $\alpha, p$ ) reactions.

Gentry (8) has shown that none of the above alternatives are very probable, implying that the giant halos may well represent unknown  $\alpha$ -radioactivity. In this respect the giant halos in cordierite reported (and photographed) by Krishnan & Mahadevan (39) are very significant. The "Th" giant halos they report may be due to the low abundance  $\alpha$ s from  $^{212}\text{Po}$ . In contrast the "U" giant halos correspond to an  $E_a$  of about 9.5 MeV and cannot be explained on the basis of a low-abundance  $^{238}\text{U}$  decay series  $\alpha$ -emitter.

It has been suggested (24) that high spin or shape isomers that exhibit high energy  $\alpha$ -decay may be responsible for the giant halos (8), a hypothesis that is presently under investigation (Gentry et al 40). There is practically nothing to suggest a superheavy element connection (8).

Figure 2c shows a dark, overexposed and partially reversed (near the inclusion) Th halo in a sample of ordinary biotite. Figure 2d, e shows Th halos in the Madagascar mica. Here the  $\alpha$ -dose has created a lighter rather than a darker coloration. Figure 2f shows a U halo in the same mica. The ring structure in Figure 2l, e, f is missing, of course, due to the large inclusions. Figure 2g shows a 65-mm giant halo close to two

very light Th halos. Figure 2h exhibits a giant halo of about 90-mm radius. If produced by high energy  $\alpha$ s, the halos in Figure 2g, h correspond to an  $E_\alpha$  of 11.6 and 14 MeV respectively.

### Mass Analysis of Halo Inclusions

The preceding sections have presented data on unusual size halos that may well have important implications for nuclear science and cosmology. If, for example Po halos did originate with isomers that were long-lived  $b$ -decaying precursors of Po, then some of these isomers may represent extinct natural radioactivity (Kohman 41) and hence will be of cosmological significance. Possibly the isomer hypothesis for the giant halos may bear similar implications. Now the above inferences have been deduced solely on the basis of halo ring structure. Clearly the variant halo inclusions themselves contain another important source of information about the radionuclides which generated such halos. However, the small inclusion size effectively prevents use of ordinary mass spectrometric techniques.

To circumvent these problems Gentry has utilized the recently developed ion microprobe mass spectrometer (Anderson & Hinthorne 42) for in situ mass analysis of even the smallest halo inclusions (8, 28, 40). Many U and Th inclusion were analyzed to obtain isotopic data against which the results from the variant halos may be compared. The most important specific application thus far has been the analysis of Po halo inclusions.

Because the Po halos shown in Figure 1p, q, r, s, t all initiate with Po isotopes that terminate with  $^{206}\text{Pb}$ , these inclusions should reflect an excess of this Pb isotope; further because ring structure and fission track analysis show only small amounts, if any, of U, mass analysis of such Po halo inclusions should be consistent with these observations as well. A mixed type Po halo such as in Figure 1u (or Figure 1o) would be expected to exhibit excesses of both  $^{206}\text{Pb}$  (from

$^{210}\text{Po}$  decay) and  $^{208}\text{Pb}$  (from  $^{212}\text{Po}$  decay). If  $^{211}\text{Bi}$  halos have been properly identified (30), an excess of the decay product  $^{207}\text{Pb}$  should exist in these inclusions. Generally then, while any given Po halo inclusion might have initially contained varying amounts of the different Po isotopes (or their  $b$ -decaying precursors), halo rings would develop only if  $\sim 10^8$  atoms of a specific nuclide were present. This implies Po isotope ratios may be variable even when examining different Po halos of the same general type. (In principle this is similar to the case where varying amounts of Th are found in halo inclusions around which only U rings appear.)

Specifically ion probe analyses have shown one  $^{210}\text{Po}$  halo inclusion that contained Pb without any detectable  $^{204}\text{Pb}$ , U, or Th; the  $^{206}\text{Pb}/^{207}\text{Pb}$  ratio was  $\approx 20$ . Absence of U and Th means this Pb was not radiogenically derived from these elements; absence of  $^{204}\text{Pb}$  means this Pb cannot be primordial or common Pb as those terms are usually defined. Briefly, while these values are inexplicable on the basis of any heretofore known types of Pb, they definitely agree with a Pb type derived from Po decay independent of U or Th.

In other Po inclusions the  $^{206}\text{Pb}/^{207}\text{Pb}$  ratio has been determined as ca 10, 12, 18, 22, 25, 40, 62, and 80. The theoretical maximum possible radiogenic  $^{206}\text{Pb}/^{207}\text{Pb}$  ratio, based on an instantaneous production of Pb from normal isotopic U decay, is 21.8. Therefore,  $^{206}\text{Pb}/^{207}\text{Pb}$  ratios greater than 21.8 not only reflect the existence of a unique type of Pb, but in a different way confirm the existence of Pb derived from Po decay independent of the normal U decay chain (28, 40).

Several of the Po halo inclusions described above were concurrently analyzed for the presence of the postulated Po isomers but with negative results so far (40). Gentry is continuing the search using different types of Po halos taken from rocks from several geological epochs. In closing we note successful application in obtaining the Pb isotope ratios gives promise that the mysteries of the other variant halos will not long remain unsolved.

### Literature Cited

1. Joly, J. 1907. *Phil. Mag.* 13:381-83
2. Mügge, O. 1907. *Zentralbl. Mineral.* 1907:397-99 (See also Oak Ridge Nat. Lab. transl. ORNL-tr-757)
3. Rutherford, F. 1910. *Phil. Mag.* 19: 192- 94
4. Joly, J., Rutherford, E. 1913. *Phil. Mag.* 25: 644-5 7
5. Fleischer, R. L., Price, P. B., Walker, R. M. 1965. *Science* 149:383-93
6. Gentry, R. V. 1968. *Science* 160: 1228-30
7. Picciotto, F. E., Deutsch, S. 1960. *Pleochroic Halos*. Rome: Comitato Nazionale per l'Energia Nucleare
8. Gentry, R. V. 1970. *Science* 169:670-73
9. Hövermann, G. 1912. *Neues Jahrb. Mineral. Geol. Palaeontol. Beilageband Bd. 34:* 321 400 (See also ORNL-tr-923)
10. Poole, J. H. J. 1928. *Phil. Mag.* 5: 132- 41; Idem. 1928. *Phil. Mag.* 5:444
11. Przibram, K. 1956. *Irradiation Colors and Luminescence*. London: Pergamon
12. Ramdohr, P. 1933. *Neues Jahrb. Mineral. Beilageband Abt. A 67:* 5365 (See also ORNL-tr-701); Ramdohr, p. 1957. *Abh. Deut. Akad. Wiss. Berlin. Kl. Chem. Geol. Biol.* 2: 1-17 (See also ORNL-tr-755); Ramdohr, P. 1960. *Geol. Rundsch.* 49: 253-63 (See also ORNL-tr-758)
13. Stark, M. 1936. *Chemie Erde X:566—630* (See also ORNL-tr-700)
14. Jedwab, J. 1966. *Advan. Chem. Ser.* 55:119-30
15. Joly, J. 1917. *Phil. Trans. Roy. Soc. London Ser. A* 217:51-79; Idem. 1917. *Nature* 99:456-58, 476-78; Idem. 1923. *Proc. Roy. Soc. London Ser. A* 102:682- 705; Idem. 1924. *Nature* 114:160-64
16. Lingen, J. S. van der 1926. *Zentralbl. Mineral. Aht. A*, 177-83 (See also ORNL-tr-699)
17. Wiman, E. 1930. *Bull. Geol. Inst. Univ. Uppsala* 23: 1-170
18. Iimori, S., Yoshimura, J. 1926. *Sci. Pap. Inst. Phys. Chem. Res.* 5: 11-23
19. Kerr-Lawson, D. E. 1927. *Univ. Toronto Stud. Geol. Ser.* 24: 54-71; Idem. 1928. *Univ. Toronto Stud. Geol. Ser.* 27: 15-27
20. Henderson, G. H., Bateson, S., 1934. *Proc. Roy. Soc. London Ser. A* 145: 563- 81; Henderson, G. H., Turnbull, L. G. 1934. *Proc. Roy. Soc. London Ser. A* 145:582—98; Henderson, G. H., Mushkat, C. M., Crawford, D. P. 1934. *Proc. Roy. Soc. London Ser. A* 158: 199-211

**Reprinted from**  
**ANNUAL REVIEW OF NUCLEAR SCIENCE**  
**Volume 23, 1973**  
**Copyright 1973, All rights reserved.**

21. Hirschi, H. 1920. *Vierteljahresschr. Naturforsch. Ges. Zuerich* 65: 209-47 (See also ORNL-tr-702); Idem. 1924. *Naturwissenschaften* 12: 939-40 (See also ORNL-tr-708)
22. Gudden, B. 1924. *Z. Phys.* 26:110-16
23. Schilling, A. 1926. *Neues Jahrb. Mineral. Abh. A* 53:241-65 (See also ORNL-tr-697)
24. Gentry, R. V. Unpublished
25. Mahadevan, C. 1927. *Indian J. Phys.* 1:445-55
26. Hutton, C. O. 1947. *Am. J. Sci.* 245: 154-57
27. Snetsinger, K. G. 1967. *Am. Mineral* 52: 1901-3
28. Gentry, R. V. 1971. *Science* 173:727-31
29. Holmes, A. 1931. *Bull. Nat. Res. Counc* 80:124-460
30. Gentry, R. V. 1967. *Nature* 213:487-89
31. Spector, R. M. 1971. *Phys. Rev. A* 5: 1323-27
32. Henderson, G. H., Sparks, F. W. 1939. *Proc. Roy. Soc. London Ser. A* 173:238- 49; Henderson, G. H. 1939. *Proc. Roy. Soc. London Ser. A* 173 :250-64
33. Huang, W. H., Walker, R. M. 1967. *Science* 155: 1103-6
34. Laemlein, G. G. 1945. *Nature* 155:724-25
35. Brukl, A., Hernegger, F., Hilbert, H. 1951. *Oesterr. Akad. Wiss. Math. Naturwiss. Kl. Sitzungsber. Aht. hA* 160: 129-46
36. Schintlmeister, J., Hernegger, F. 1940. *Ger. Rep. G-55, Part I*; Idem. 1941. *Ger.Rep. G-112, Part II*; Schintlmeister, J. 1941. *Ger. Rep. G-111, Part 111*; Schintlmeister, J. 1942. *Ger. Rep. G-186*
37. Gentry, R. V. 1967. *Earth Planetary Sci. Lett.* 1:453-54
38. Höpfe, G. 1959. *Geol. Fören. Stockholm Förh.* 81:485-94 (See also ORNL-tr-756)
39. Krishnan, M. S., Mahadevan, C. 1930. *Indian J. Sci.* 5:669-80
40. Gentry, R. V., Cristy, S. S., McLaughlin J. F., McHugh, J. A. 1973. *Nature* 244 282
41. Kohman, T. p. 1961. *J. Chem. Educ.* 38 73-82
42. Anderson, C. A., Hinthorne, J. R. 1972 *Science* 175:853-60